

## Semi-active Sliding Mode Control of Vehicle Suspension with Magneto-rheological Damper

ZHANG Hailong<sup>1,2</sup>, WANG Enrong<sup>2,\*</sup>, ZHANG Ning<sup>1</sup>, MIN Fuhong<sup>2</sup>, SUBASH Rakheja<sup>3</sup>, and SU Chunyi<sup>3</sup>

<sup>1</sup> School of Physics and Technology, Nanjing Normal University, Nanjing 210042, China

<sup>2</sup> School of Electric and Automation Engineering, Nanjing Normal University, Nanjing 210042, China

<sup>3</sup> Department of Mechanical Engineering, Concordia University, Montreal H3G 1M8, Canada

Received May 29, 2013; revised September 11, 2014; accepted September 18, 2014

**Abstract:** The vehicle semi-active suspension with magneto-rheological damper(MRD) has been a hot topic since this decade, in which the robust control synthesis considering load variation is a challenging task. In this paper, a new semi-active controller based upon the inverse model and sliding mode control (SMC) strategies is proposed for the quarter-vehicle suspension with the magneto-rheological (MR) damper, wherein an ideal skyhook suspension is employed as the control reference model and the vehicle sprung mass is considered as an uncertain parameter. According to the asymptotical stability of SMC, the dynamic errors between the plant and reference systems are used to derive the control damping force acquired by the MR quarter-vehicle suspension system. The proposed modified Bouc-wen hysteretic force-velocity ( $F-v$ ) model and its inverse model of MR damper, as well as the proposed continuous modulation (CM) filtering algorithm without phase shift are employed to convert the control damping force into the direct drive current of the MR damper. Moreover, the proposed semi-active sliding mode controller (SSMC)-based MR quarter-vehicle suspension is systematically evaluated through comparing the time and frequency domain responses of the sprung and unsprung mass displacement accelerations, suspension travel and the tire dynamic force with those of the passive quarter-vehicle suspension, under three kinds of varied amplitude harmonic, rounded pulse and real-road measured random excitations. The evaluation results illustrate that the proposed SSMC can greatly suppress the vehicle suspension vibration due to uncertainty of the load, and thus improve the ride comfort and handling safety. The study establishes a solid theoretical foundation as the universal control scheme for the adaptive semi-active control of the MR full-vehicle suspension decoupled into four MR quarter-vehicle sub-suspension systems.

**Keywords:** magneto-rheological damper, vehicle suspension, multi-objective performance, semi-active sliding mode control, filtering

### 1 Introduction

The semi-active suspension with new magneto-rheological(MR) damper has become one of the most attractive technical and challenging task for improving the road vehicle suspension performances of ride comfort and handling safety, due to the contradictory controlling demand on the suspension damping for ride comfort and handling safety, as well as the adaptive robust control requirement on hysteresis and force saturation nonlinearities of MR damper and vehicle load uncertainty, etc<sup>[1]</sup>. A lot of achievements have been published about the semi-active controller syntheses of MR quarter-vehicle suspension on basis of the modern robust control schemes, to realize the robust control on the parameter uncertainties of suspension system<sup>[2-6]</sup>. YOKOYAMA, et al<sup>[7]</sup>, early

conducted the sliding mode control (SMC) policy-based semi-active control on MR quarter-vehicle suspension, by employing the proposed Bouc-wen hysteresis  $F-v$  model of the MR damper and ideal skyhook suspension system as the control reference model. Similarly, YAO, et al<sup>[8]</sup>, conducted the SMC-based semi-active controller synthesis of MR quarter-vehicle suspension, by applying the proposed polynomial hysteresis  $F-v$  model of the MR damper and its inverse model, so as to suppress the hysteresis nonlinearity of the MR damper. However, the above-mentioned two control strategies cannot achieve ideal control goal, because the employed Bouc-wen and polynomial hysteresis  $F-v$  models characterize yielded damping force in linear relationship with the control direct current, which cannot precisely formulate the direct magnetic field of the MR damper in nonlinear and saturation dependences on the control direct current. Moreover, GUO, et al<sup>[9]</sup>, proposed a neural network-based semi-active control scheme for the MR quarter-vehicle suspension, which can effectively suppress hysteresis nonlinearity, but yields a better control effect only in the

\* Corresponding author. E-mail: erwang@njnu.edu.cn

Supported by National Natural Science Foundation of China (Grant Nos. 51475246, 51277098)

low frequency band. CHOI, et al<sup>[10]</sup>, further proposed the  $H_\infty$ -based semi-active controller for the MR full-vehicle suspension, which considered the sprung mass as an uncertain parameter and achieved a better robust control effect, whereas the controller is more complicate and difficult in application, due to the strong coupling of the four MR quarter-vehicle sub-suspension systems in the full-vehicle system. The above studies have greatly improved the robust semi-active controller synthesis of the intelligent MR vehicle suspension system, but lacked for consideration of multi-objective suspension performances, such as resonance suppression, vibration isolation, road holding, hysteresis rejection and load variation adaptation, etc.

From the literature survey above-mentioned, the studies of semi-active control on MR vehicle suspension were insufficient. The authors have recently focused on the adaptive semi-active control study of MR full-vehicle suspension supported by the National Natural Science Foundation of China (51475246, 51277098) in a systematic procedure<sup>[11-17]</sup>, which establishes upon decoupling MR full-vehicle suspension into four MR quarter-vehicle sub-suspension systems, so as to achieve multi-objective suspension performances of vertical, pitch and roll motions of MR full-vehicle suspension. In Ref. [11], the preliminary design of the sliding model-following control for semi-active MR-vehicle suspension was proposed, considering the variations in the vehicle load and based upon a modified skyhook-based reference model. In this paper, the strategy of sliding model-following control is improved on to ensuring system stability and robustness. The study is still aimed at the MR quarter-vehicle suspension system and proposes an idealized skyhook reference model-based semi-active sliding mode controller (SSMC) by considering the sprung mass as an uncertain parameter. According to the dynamic errors between the plant and reference system, the acquired control damping force can be derived and further converted to the direct control current, by employing the proposed modified Bouc-wen hysteretic  $F$ - $v$  model and inverse model of the MR damper<sup>[8]</sup>. The proposed continuous modulation (CM) filtering algorithm without phase shift are further utilized to modulate the obtained direct control current with high precision and smooth continuity, for the purpose of decreasing the harsh mechanical rub of the piston motion and thus extending the service life of MR damper. Moreover, the time and frequency domain responses of the proposed SSMC-based MR quarter-vehicle suspension are compared with those of the passive quarter-vehicle suspension, under the varied amplitude harmonic, the rounded pulse and the real road measured random excitations, in which the sprung and unsprung mass displacement accelerations, the suspension travel and the tire dynamic force are chosen as evaluated responses.

## 2 Dynamic Model of MR Quarter-vehicle Suspension System

In Fig. 1, a common dynamic model of MR quarter-vehicle suspension system<sup>[14-16]</sup> is plotted, which involves main vehicle components such as the car body, suspension spring, MR damper and wheel, etc. Amongst, only the MR damper has strong force hysteresis and saturation nonlinearities. The other components have been processed in linearization.  $m_s$  and  $m_u$  are defined as the sprung and unsprung masses.  $k_s$ ,  $i_d$  and  $F_d$  represent the suspension stiffness, direct drive current and the yielded damping force of the MR damper.  $k_t$  and  $c_t$  denote equivalent stiffness and damping coefficient of the tire, and  $x_i$ ,  $x_s$  and  $x_u$  are defined as the road excitation, vertical displacements of the sprung and unsprung masses, respectively. The dynamic equation is formulated as

$$\begin{cases} m_s \ddot{x}_s + k_s(x_s - x_u) + F_d - m_s g = 0, \\ m_u \ddot{x}_u + F_t - k_s(x_s - x_u) - F_d - m_u g = 0, \end{cases} \quad (1)$$

where  $F_t$  is defined as the tire dynamic force, and

$$F_t = \begin{cases} k_t(x_u - x_i) + c_t(\dot{x}_u - \dot{x}_i), & x_u - x_i > 0, \\ 0, & x_u - x_i < 0. \end{cases} \quad (2)$$

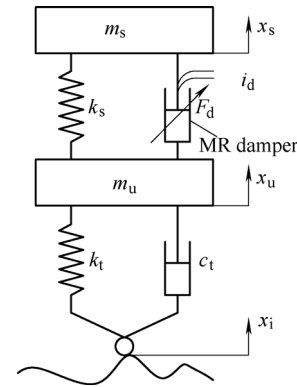


Fig. 1. Dynamic model of MR quarter-vehicle suspension

## 3 Modified Bouc-wen Hysteresis $F$ - $v$ Model and Inverse Model

The original Bouc-wen hysteresis  $F$ - $v$  model proposed by SPENCER, et al<sup>[18]</sup> can precisely formulate the hysteretic nonlinearity of the MR damper, whereas the model lacks precision in describing nonlinear and saturation dependences of the magnetic field yielded by the direct drive current in the MR damper, because the model linear function is utilized to formulate the control relationship between the damping force and direct drive current<sup>[19]</sup>. Therefore, a sigmoid-based nonlinear direct current control function proposed by the authors is applied

to modify the proposed original Bouc-wen hysteresis  $F$ - $v$  model, such that the modified Bouc-wen hysteresis  $F$ - $v$  model can not only precisely describe the nonlinear hysteresis characteristic, but also precisely describe the saturated nonlinear direct current control characteristic of the MR damper<sup>[13]</sup>.

$$F_d = f(i_d) = c(i_d)F_h(v_r), \quad (3)$$

$$c(i_d) = 1 + \frac{k_2}{1 + \exp(-a_0(i_d + I_0))} - \frac{k_2}{1 + \exp(-a_0 I_0)}, \quad (4)$$

$$F_h(v_r) = c_1 \dot{y} + k_1(x - x_0), \quad (5)$$

$$\begin{cases} \dot{x} = x_s - x_u, \\ \dot{y} = \frac{1}{c_0 + c_1} [\alpha z + c_0 \dot{x} + k_0(x - y)], \\ \dot{z} = -\gamma |\dot{x} - \dot{y}| z |z|^{n-1} - \beta (\dot{x} - \dot{y}) |z|^n + A(\dot{x} - \dot{y}), \end{cases} \quad (6)$$

where  $i_d$  and  $I_m$  express the direct current and its maximum value for driving the MR damper,  $0 \leq i_d \leq I_m$ ,  $c(i_d)$  denotes the saturated nonlinear direct current control function proposed by the authors,  $c(i_d) \geq 1$ , when  $i_d=0$ ,  $c(i_d)=1$ .  $F_h(v_r)$  denotes yielded passive damping force with hysteresis depending on the piston relative displacement velocity  $v_r$  of the MR damper, when  $i_d=0$ .  $x$  expresses the piston travel of MR damper,  $y$  and  $z$  are inner variables without units, and  $k_0, k_1, k_2, a_0, I_0, \alpha, \beta, \gamma, c_0, c_1, n, A, x_0$  are constants, respectively. It is not difficult to find that the modified Bouc-wen hysteresis  $F$ - $v$  model decouples direct current control function and hysteron as shown in Eq. (3). Its inverse model can be easily derived as follows:

$$i_d = f^{-1}(F_d) = \begin{cases} -I_0 - \frac{1}{a_0} \left( \frac{(k_2 - F_d / F_h + 1) \exp(-a_0 I_0) - F_d / F_h + 1}{(F_d / F_h - 1)(1 + \exp(-a_0 I_0)) + k_2} \right), & F_d \cdot F_h > 0, \\ 0, & F_d \cdot F_h \leq 0. \end{cases} \quad (7)$$

As shown in Fig. 2, A CARRERA<sup>TM</sup> MagneShock MR damper of the vehicle suspension is employed in this study, which permits maximum control direct current 0.5 A at 12 V<sup>[14]</sup>. On basis of the really measured characteristic data of MR damper, the model parameters are identified as  $k_0=184.1$ ,  $k_1=1528.1$ ,  $k_2=10.092$ ,  $a_0=7.526$ ,  $I_0=0.069$ ,  $\alpha=20$ ,  $\beta=373.7$ ,  $\gamma=233$ ,  $\beta=849.1$ ,  $\gamma=8816.9$ ,  $c_0=1368.7$ ,  $c_1=6222.7$ ,  $n=2$ ,  $A=20.6$ ,  $x_0=-0.004$ <sup>[13]</sup>. In Fig. 3, it shows the comparison of the modified Bouc-wen hysteresis  $F$ - $v$  model and the measured data of employed candidate MR damper, under the harmonic excitation with amplitude 12.5 mm at 1.5 Hz and different direct drive current (0–0.4 A), which exhibits ideal coordination.



Fig. 2. CARRERA<sup>TM</sup> MR damper

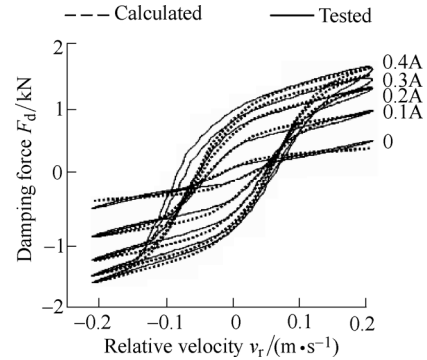


Fig. 3. Result comparison of modified Bouc-wen hysteresis  $F$ - $v$  model and measured data of candidate MR damper

#### 4 Semi-active Sliding Mode Controller Synthesis

The dynamic systems of MR quarter-vehicle suspension exactly as shown in Fig. 1 and the modified skyhook reference model are respectively illustrated in Figs. 4(a) and 4(b), which are used to synthesize semi-active sliding mode controller (SSMC) by motion tracking of the vehicle suspension sprung mass  $m_s$  to the reference model sprung mass  $m_{s0}$ .

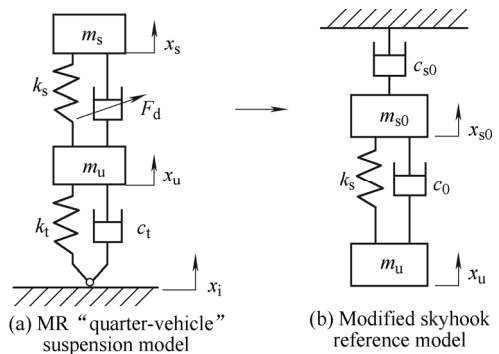


Fig. 4. Semi-active sliding mode controller design using skyhook reference model

##### 4.1 Sliding mode controller synthesis

According to the sliding mode control (SMC) synthesis rule, an asymptotically stable sliding mode state can be derived from dynamic errors between the MR quarter-vehicle suspension system and the modified

skyhook reference model system<sup>[7, 11]</sup>. In the skyhook reference model shown in Fig. 4(b), the unsprung mass displacement  $x_u$  of MR quarter-vehicle suspension can be directly used as excitation input of the skyhook reference model system, because the real tire stiffness is generally 5 times of the suspension spring stiffness. As a result, dynamic equation of the skyhook reference model system can be formulated as

$$m_{s0}\ddot{x}_{s0} + c_0(\dot{x}_{s0} - \dot{x}_u) + c_{s0}\dot{x}_{s0} + k_s(x_{s0} - x_u) = 0, \quad (8)$$

where  $m_{s0}$  is reference model sprung mass, which equals empty load sprung mass of the MR quarter-vehicle suspension,  $c_{s0}$  and  $x_{s0}$  are skyhook damping coefficient and reference model sprung mass displacement, as well  $c_0$  and  $k_s$  denote damping coefficient and spring stiffness of the passive quarter-vehicle suspension, respectively.

For the MR quarter-vehicle suspension system, we define the sliding mode surface as

$$s = \dot{e}_s(t) + \lambda e_s(t), \quad (9)$$

where  $\lambda > 0$  denotes the convergence rate of sliding mode surface,  $e_s(t) = x_s(t) - x_{s0}(t)$  expresses the sprung mass vertical displacement errors between both the dynamic systems of MR quarter-vehicle suspension and the skyhook reference model, and  $e(t)$  equals 0 when  $t$  tends to infinite.

Furthermore, we define the Lyapunov function as  $V = s^2/2$ . To guarantee that the system state asymptotically switches to the sliding surface, it is defined that

$$\dot{V} = \dot{s}s \leq -\phi|s|, \quad (10)$$

where  $\phi$  is a positive constant.

Neglecting gravity action in Eq. (1), we obtain

$$\ddot{x}_s = \frac{1}{m_s}[-k_s(x_s - x_u) - F_d]. \quad (11)$$

Combining Eq. (9) and Eq. (11), we further obtain

$$\dot{s} = \frac{1}{m_s}[-k_s(x_s - x_u) - F_d] - \ddot{x}_{s0} + \lambda \dot{e}_s(t). \quad (12)$$

According to the stability condition of sliding mode control strategy,  $\dot{s}s = 0$ , the idealized control damping force  $F_{d0}$  of MR quarter-vehicle suspension can be derived from Eq. (12) as

$$F_{d0} = -k_s(x_s - x_u) - m_{s0}\ddot{x}_{s0} + m_{s0}\lambda \dot{e}_s. \quad (13)$$

To ensure that yielded damping force  $F_d$  of the MR damper can fast track its idealized control damping force  $F_{d0}$ , we define the control damping force  $F_c$  by employing the switch control policy as

$$F_c = F_{d0} - K \operatorname{sgn}(s), \quad (14)$$

where  $K$  is the gain of SMC to be further derived, and  $\operatorname{sgn}(s)$  is sign function which takes  $-1$  and  $1$  when  $s \leq 0$  and  $s > 0$ , respectively.

According to  $\dot{V} = \dot{s}s$ , we use  $F_c$  to replace  $F_d$  in Eq. (12) substitute it into  $\dot{V} = \dot{s}s$  and thus obtain

$$\dot{V} = \left( -\frac{k_s}{m_s}x_s + \frac{k_s}{m_s}x_u - \frac{F_c}{m_s} - \ddot{x}_{s0} + \lambda \dot{e}_s \right) s. \quad (15)$$

By further substituting Eq. (14) into Eq. (15), we get

$$\dot{V} = \left[ -\frac{k_s}{m_s}x_s + \frac{k_s}{m_s}x_u - \frac{F_{d0} - K \operatorname{sgn}(s)}{m_s} - \ddot{x}_{s0} + \lambda \dot{e}_s \right] s. \quad (16)$$

Combining Eqs. (13) and (16), we obtain

$$\dot{V} = \left[ \left( \frac{1}{m_s} - \frac{1}{m_{s0}} \right) (-k_s x_s + k_s x_u - F_{d0}) + \frac{K}{m_s} \operatorname{sgn}(s) \right] s. \quad (17)$$

According to the Lyapunov stability condition of SMC, we substitute Eq. (17) into Eq. (10) and obtain

$$\left[ \left( \frac{1}{m_s} - \frac{1}{m_{s0}} \right) (-k_s x_s + k_s x_u - F_{d0}) + \frac{K}{m_s} \operatorname{sgn}(s) \right] s \leq -\phi|s|. \quad (18)$$

Considering  $|s| = s \cdot \operatorname{sgn}(s)$ , Eq. (18) can be further expressed as

$$\left[ \left( \frac{1}{m_s} - \frac{1}{m_{s0}} \right) (-k_s x_s + k_s x_u - F_{d0}) + \frac{K}{m_s} \operatorname{sgn}(s) \right] s \leq -\phi \cdot s \cdot \operatorname{sgn}(s), \quad (19)$$

for  $s \geq 0$ , Eq. (19) can be simplified as

$$K \leq -m_s \phi + \left( 1 - \frac{m_s}{m_{s0}} \right) (k_s x_s - k_s x_u + F_{d0}), \quad (20)$$

for  $s < 0$ , Eq. (19) can be simplified as

$$K \leq -m_s \phi + \left( 1 - \frac{m_s}{m_{s0}} \right) (-k_s x_s + k_s x_u - F_{d0}). \quad (21)$$

Considering that the real load of a vehicle is often variable, we define  $\eta$  as the variation rate of vehicle sprung mass  $m_s$  to its empty load sprung mass  $m_{s0}$ , i.e.,  $\eta = m_s/m_{s0} \geq 1$ . As a result, by comprehensively considering Eqs. (20) and (21), we choose  $K$  of SMC as

$$K = -m_{s0} \eta \phi - (\eta - 1) (|F_{d0}| + k_s |x_s| + k_s |x_u|). \quad (22)$$

Furthermore, the saturation function  $sat(s)$  is utilized to replace the sign function  $sgn(s)$  in Eq. (14) for avoiding chattering oscillation occurred in the system, and takes  $s/\varepsilon$  and  $sgn(s)$  when  $|s| \leq \varepsilon$  and  $|s| > \varepsilon$ , respectively. Such that Eq. (14) can be rewritten as

$$F_c = F_{d0} - Ksat(s). \quad (23)$$

where  $\varepsilon$  is a positive constant.

#### 4.2 Proof of proposed sliding mode controller stability

In section 4.1, the proposed SMC is formulated in Eqs. (23), (22) and (13), which aims at calculating the acquired control damping force  $F_c$  of the MR quarter-vehicle suspension system, and it is necessary to prove that the sliding surface of the proposed SMC can tend towards asymptotical stability.

By substituting Eq. (22) into Eq. (17), we obtain

$$\dot{V} = \left[ \frac{\eta-1}{\eta m_{s0}} (F_{d0} + k_s x_s - k_s x_u) - \frac{(\eta-1)(|F_{d0}| + k_s |x_s| + k_s |x_u|)}{\eta m_{s0}} sgn(s) - \phi sgn(s) \right] s, \quad (24)$$

for  $s \geq 0$ , Eq. (24) can be rewritten as

$$\dot{V} = \left[ \frac{\eta-1}{\eta m_{s0}} (F_{d0} + k_s x_s - k_s x_u) - \frac{(\eta-1)(|F_{d0}| + k_s |x_s| + k_s |x_u|)}{\eta m_{s0}} - \phi \right] s. \quad (25)$$

Because  $\eta > 1$ ,  $\phi$ ,  $m_{s0}$  are positive constants, such that

$$\frac{(\eta-1)}{\eta m_{s0}} (F_{d0} + k_s x_s - k_s x_u) - \frac{(\eta-1)(|F_{d0}| + k_s |x_s| + k_s |x_u|)}{\eta m_{s0}} - \phi < 0,$$

and thus  $\dot{V} < 0$ .

Similarly, for  $s < 0$ , Eq. (24) can be rewritten as

$$\dot{V} = \left[ \frac{\eta-1}{\eta m_{s0}} (F_{d0} + k_s x_s - k_s x_u) + \frac{(\eta-1)(|F_{d0}| + k_s |x_s| + k_s |x_u|)}{\eta m_{s0}} + \phi \right] s, \quad (26)$$

obviously,

$$\frac{(\eta-1)}{\eta m_{s0}} (F_{d0} + k_s x_s - k_s x_u) + \frac{(\eta-1)(|F_{d0}| + k_s |x_s| + k_s |x_u|)}{\eta m_{s0}} + \phi > 0,$$

and thus  $\dot{V} < 0$ .

Consequently, it does not matter whether  $s \geq 0$  or  $s < 0$ , the proposed SMC can guarantee asymptotical stability of the controlled MR quarter-suspension system.

#### 4.3 SSMC-based MR quarter-vehicle suspension system

It is required to obtain the direct control current  $i_c$  converted from the control damping force  $F_c$  in Eq. (23) for driving MR damper, because the MR damper is a semi-active smart device. Applying the proposed MR damper inverse model in Eq. (7), we define logic condition  $z_c = F_c F_h$ , and thus obtain  $i_c = f^{-1}(F_c)$  when  $z_c > 0$  and  $i_c = 0$  when  $z_c \leq 0$ . However, since the sharp discontinuous variation of the converted direct control current  $i_c$  exists around the logic condition  $z_c = 0$ , which may generate the harmful shock on the MR damper, we further apply the proposed continuous modulation (CM) algorithm<sup>[8]</sup> to filter the direct control current  $i_c$ , and hence obtain direct drive current  $i_d$ , which has smooth continuity and high precision. Meanwhile, it can greatly decrease harsh mechanical rub of the piston motion and thus extend the service life of MR damper.

$$i_d = M_c(p_c, \zeta_c, z_c) i_c, \quad (27)$$

$$M_c(p_c, \zeta_c, z_c) = \frac{1+p_c}{2} + \frac{2}{\pi} \left[ p_c (z_c \geq 0 \cup z_c < 0) - \frac{1+p_c}{2} \right] |\arctan(\zeta_c z_c)|, \quad (28)$$

where the continuous modulation algorithm  $M_c(p_c, \zeta_c, z_c)$  is an algebraic function differing from traditional filter and will not yield any phase shift, herein,  $p_c$  is asymmetric coefficient depending on semi-active control law,  $0 \leq p_c \leq 1$ ,  $\zeta_c$  is smooth factor,  $\zeta_c > 0$ , and the logic condition  $p_c(z_c > 0 \cup z_c \leq 0)$  is defined to take a small value of  $p_c$  when  $z_c > 0$  and take  $p_c = 1$  when  $z_c \leq 0$ .

Consequently, the proposed SSMC can be finally formulated as

$$\begin{cases} i_d = M_c(p_c, \zeta_c, z_c) f^{-1}(F_c), \\ F_c = F_{d0} - Ksat(s), \\ K = -m_{s0} \eta \phi - (\eta-1)(|F_{d0}| + k_s |x_s| + k_s |x_u|), \\ F_{d0} = -k_s (x_s - x_u) - m_{s0} \ddot{x}_{s0} + m_{s0} \lambda \dot{e}_s. \end{cases} \quad (29)$$

The proposed SSMC-based MR quarter-vehicle suspension system can be realized by using following schematic diagram, as shown in Fig. 5. It is not difficult to find that the proposed SSMC can be easily realized in real engineering application, because it acquires only in-time measured vertical motion displacements  $x_s$  and  $x_u$  of the vehicle sprung and unsprung masses with reference to road surface, and other variables can be calculated from the system model. Moreover, the proposed inverse model-based SSMC has merits of effectively suppressing

the hysteresis nonlinearity of MR damper, which may affect stability of the controlled MR suspension system.

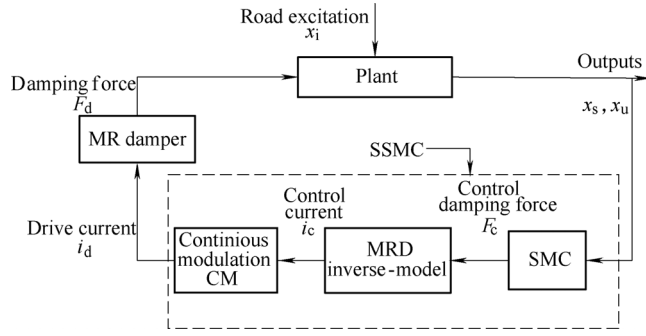


Fig. 5. Schematic diagram of SSMC-based MR quarter-vehicle suspension system

### 5 Performance Analysis of SSMC-based MR Quarter-vehicle Suspension

For evaluating the effectiveness of the proposed SSMC-based MR quarter-vehicle suspension in enhancing multi-objective suspension performances, the Matlab/Simulink is employed to build up a simulation platform, and the result comparisons are conducted between the SSMC-based MR quarter-vehicle suspension and the passive quarter-vehicle suspension in which the MR damper is replaced with a passive damper  $c_s$ , under harmonic, rounded pulse and measured road random excitations. The model parameters of MR quarter-vehicle suspension shown in Fig. 1 are listed in Table 1<sup>[11]</sup>, and parameters of the SSMC are chosen as  $\lambda=1.5$ ,  $\eta=1.5$ ,  $\phi=0.05$ ,  $\varepsilon=1$ ,  $p_c=0.66$ ,  $\zeta_c=20$ .

Table 1. Parameters of the SSMC-based MR quarter-vehicle suspension system

Parameter	Value
Sprung mass $m_s$ /kg	563
Unsprung mass $m_u$ /kg	90
Suspension spring stiffness $k_s$ /(kN • m <sup>-1</sup> )	57
Passive suspension damping coefficient $c_s$ /(N • s • m <sup>-1</sup> )	2500
Tire stiffness $k_t$ /(kN • m <sup>-1</sup> )	285
Tire damping coefficient $c_t$ /(N • s • m <sup>-1</sup> )	0
Reference model sprung mass $m_{s0}$ /kg	563
Skyhook damping coefficient $c_{s0}$ /(kN • s • m <sup>-1</sup> )	4.5
Passive damping coefficient $c_0$ /(kN • s • m <sup>-1</sup> )	2.5

#### 5.1 Force tracking ability

The proposed SSMC-based MR quarter-vehicle suspension system is realized through forcing the yielded damping force of MR damper to track the control damping force calculated from SSMC in real time. In Fig. 6, it is shown the time domain response comparisons of yielded control current and the damping force of SSMC-based MR quarter-vehicle suspension system, under a harmonic excitation with amplitude 2.5 cm at frequency 1.5 Hz. The comparison between the direct drive current  $i_d$  and the control current  $i_c$  of the MR damper, as shown in Fig. 6(a),

aims to illustrate filtering role without phase shift of the proposed CM algorithm in Eq. (28), in which the direct control current  $i_c$  behaves serious sharp variations, while the direct drive current  $i_d$  of MR damper behaves ideal smooth continuity and holds same phase with that of  $i_c$ . Furthermore, the comparison between the yielded damping force  $F_d$  of MR damper and the control damping force  $F_c$ , as shown in Fig. 6(b), aims to illustrate the tracking ability of  $F_d$  to  $F_c$  calculated from the proposed SSMC, and the phase comparison between  $F_d$ ,  $F_c$  and yielded passive damping force  $F_h$  can reasonably explain the operation principle of the proposed inverse model control policy of MR damper in Eq. (7). The results show that when  $F_c$  and  $F_h$  are in inverse phase at 2.7 s to 2.8 s,  $i_c$  holds 0 and  $F_d$  approaches minimal magnitude of  $F_h$ , on the contrary, when  $F_c$  and  $F_h$  are in the same phase at 2.8 s to 2.9 s,  $i_c$  increases rapidly and  $F_d$  rapidly increases and accurately tracks  $F_c$ .

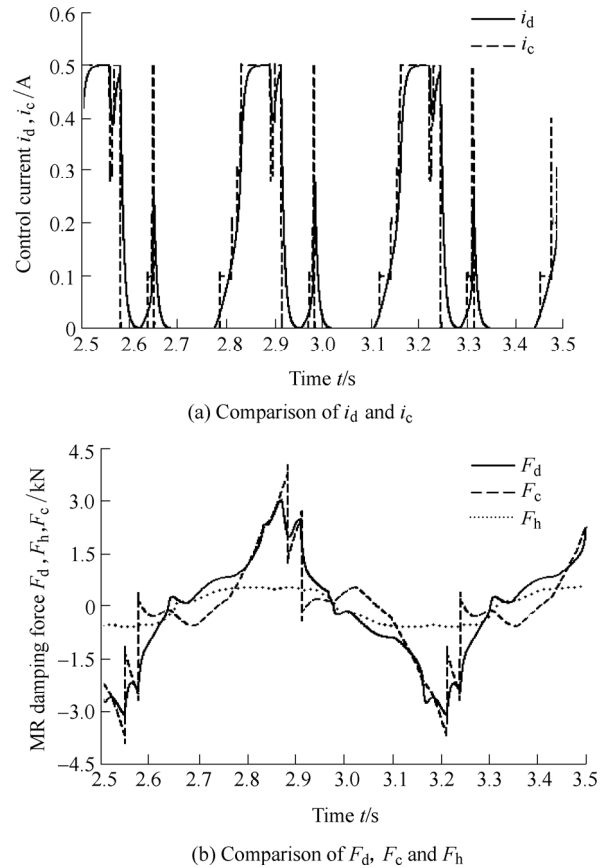


Fig. 6. Force tracking ability analysis of the SSMC-based MR quarter-vehicle suspension system

#### 5.2 Response to harmonic excitations

The harmonic excitations are usually utilized to evaluate the resonance suppression suspension performance of vehicle sprung and unsprung masses. The time domain response comparisons of SSMC-based MR and passive quarter-vehicle suspension systems under harmonic excitation is shown in Fig. 7, in which the sprung mass displacement acceleration  $a_s$ , unsprung mass displacement

acceleration  $a_u$ , suspension dynamic travel  $x_r$  and the tire dynamic force  $F_t$  are presented.

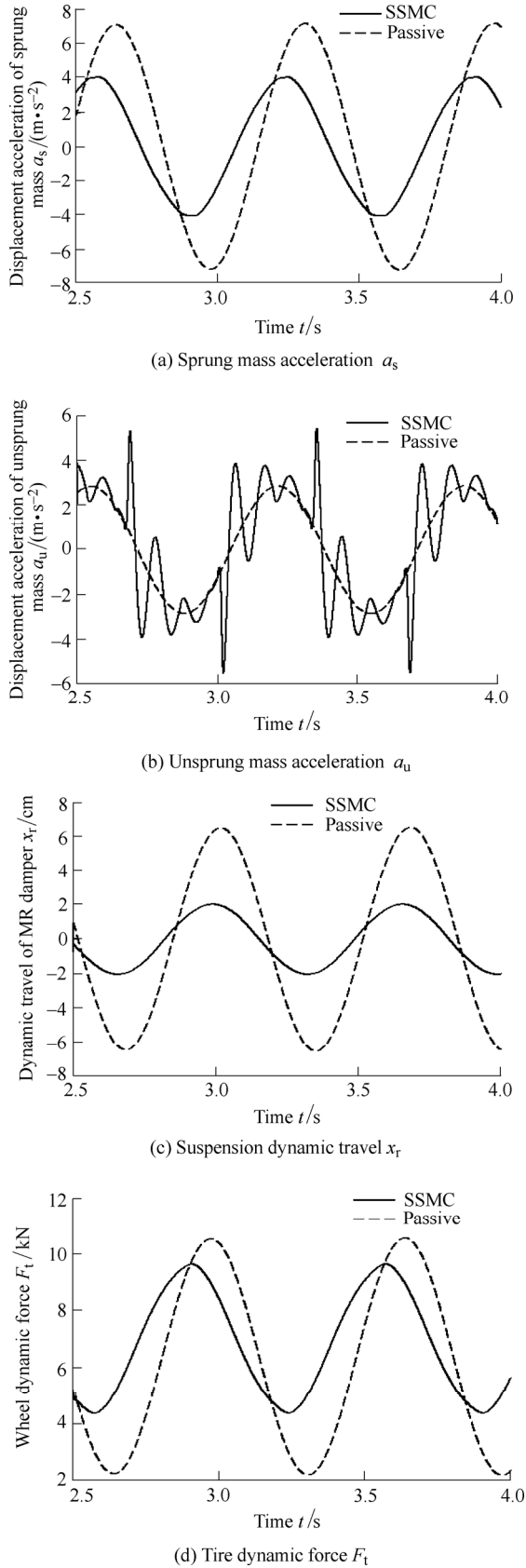


Fig. 7. Time domain response comparisons of SSMC-based MR and passive quarter-vehicle suspension systems under harmonic excitation

In Fig. 7, the harmonic excitation is of amplitude 2.5 cm

at frequency 1.5 Hz. The results illustrate that the peak magnitudes of  $a_s$ ,  $x_r$  and  $F_t$  of the SSMC-based MR quarter-vehicle suspension decrease 43%, 71% and 10% than those of the passive quarter-vehicle suspension, respectively, which greatly improve the suspension performances of sprung mass resonance suppression, limited suspension dynamic travel and road holding, and thus enhance ride comfort and handling safety of the road vehicle. Moreover, the obvious decrease of  $x_r$  magnitudes could effectively extend the service life of MR damper, by avoiding the long-term work in the limited condition. However, the improvement of above suspension performances sacrifices part of the unsprung mass resonance suppression, due to a little increase of  $a_u$  peak magnitude. Meantime, the response of  $a_u$  shows slight oscillations caused by the MR damper nonlinearity.

The frequency domain responses are usually utilized to evaluate comprehensive suspension performances of ride comfort and handling safety such as resonance suppression, vibration isolation, limited suspension dynamic travel, road holding, etc. In Fig. 8, the frequency domain response comparisons of SSMC-based MR and passive quarter-vehicle suspension systems is presented, under the harmonic excitation with varied amplitudes at road vehicle dominant frequency band<sup>[14,17]</sup>, which is formulated as

$$x_i = \begin{cases} a_m \sin(2\pi f t), & f \leq f_T, \\ a_m (f_T / f) \sin(2\pi f t), & f > f_T, \end{cases} \quad (30)$$

where the frequency band  $f$  and the cut-off frequency  $f_T$  are chosen as 0–20 Hz and 2.1 Hz, respectively, and the system evaluation indexes are chosen as the sprung mass displacement acceleration transmissibility  $T_{as}$ , unsprung mass displacement acceleration transmissibility  $T_{au}$ , suspension dynamic travel transmissibility  $T_{dr}$  and the tire dynamic load coefficient  $DLC$ <sup>[14]</sup>. It is not difficult to find that peak values of  $T_{as}$  and  $T_{dr}$  of the SSMC-based MR quarter-vehicle suspension decrease 42% and 50% than those of the passive quarter-vehicle suspension, in the low frequency band around sprung mass resonance frequency 1.5 Hz, while magnitudes of  $T_{au}$  and  $DLC$  only increase slightly, and thus effectively improves the suspension performance of the sprung mass resonance suppression<sup>[20]</sup>. Similarly, magnitudes of  $T_{au}$ ,  $T_{dr}$  and  $DLC$  of the SSMC-based MR quarter-vehicle suspension show obvious decreases than those of the passive quarter-vehicle suspension around unsprung mass resonance frequency 9.8 Hz, while  $T_{as}$  scarcely has no change, which benefits to improve the handling safety suspension performance of road vehicle. Moreover, in the middle frequency band of 3–8 Hz, magnitudes of  $T_{au}$  and  $T_{dr}$  and magnitudes of  $T_{au}$  and  $T_{dr}$  of the SSMC-based MR quarter-vehicle suspension show obvious decreases and slightly increases than those of the passive quarter-vehicle suspension, respectively, which scarify part of the vibration isolation suspension performance. In a word, the SSMC-based MR

quarter-vehicle suspension resolves the contradictory control requirement on suspension damping with a compromise scheme, and manifests ideal multi-objective suspension performances than the traditional passive quarter-vehicle, in view of the road vehicle dominant frequency band 0–20 Hz.

### 5.3 Response to rounded pulse excitations

The transient responses are usually employed to evaluate the shock suspension performance when vehicle encounters poor road conditions such as hills or hollows. Herein, the rounded pulse signal emulating road shock excitation is used to replace the traditional step input signal and is formulated as<sup>[15]</sup>

$$x_i = 0.25a_m e^2 (\mu\omega_0 t)^2 \exp(-\mu\omega_0 t) u(t), \quad (31)$$

where parameters  $a_m$ ,  $\omega_0$ ,  $\mu$  are named amplitude, fundamental frequency and stiffness of the rounded pulse excitation, and are chosen as  $a_m=2.0$  cm,  $\omega_0=10.4$  rad/s,  $\mu=3$  in this study, respectively.

In Fig. 9, it shows the time domain transient response comparisons of SSMC-based MR and passive quarter-vehicle suspension systems, under the rounded pulse excitation, and the system evaluation indexes are selected as the sprung mass displacement acceleration  $a_s$ , unsprung mass displacement acceleration  $a_u$ , suspension dynamic travel  $x_r$  and the tire dynamic force  $F_t$ . The results illustrate that transient response steady state time of  $a_s$ ,  $x_r$  and  $F_t$  of the SSMC-based MR quarter-vehicle suspension decreases nearly 50% than those of the passive quarter-vehicle suspension, which means that the proposed inverse model based SSMC effectively suppresses hysteresis nonlinearity of the MR damper and is thus helpful to enhance controller stability and improving vehicle suspension performance, whereas, peak magnitudes of  $a_s$  and  $F_t$  slightly increase and oscillation of  $F_t$  becomes more serious, which sacrifices part of the ride comfort and road friendly suspension performances.

### 5.4 Responses to random excitations

The random excitations are usually utilized to evaluate the vehicle suspension performance in much more real road condition. The response power spectrum density (PSD) comparisons of SSMC-based MR and passive quarter-vehicle suspension systems are presented in Fig. 9, under the real road measured random excitation<sup>[14, 17]</sup>. Herein, vehicle motion speed is assumed as 50 km/h., and the system evaluation indexes are still selected as sprung mass displacement acceleration  $a_s$ , unsprung mass displacement acceleration  $a_u$ , suspension dynamic travel  $x_r$  and tire dynamic force  $F_t$ . It is easily found that the response PSD magnitudes of  $a_s$ ,  $a_u$ ,  $x_r$  and  $F_t$  of the SSMC-based MR quarter-vehicle suspension greatly decrease than those of the passive quarter-vehicle suspension, and thus effectively improve the ride comfort and handling safety suspension performances of the road vehicle.

## 6 Robustness Analysis of SSMC-based MR Quarter-vehicle Suspension

Synthesis of the proposed SSMC considers not only the

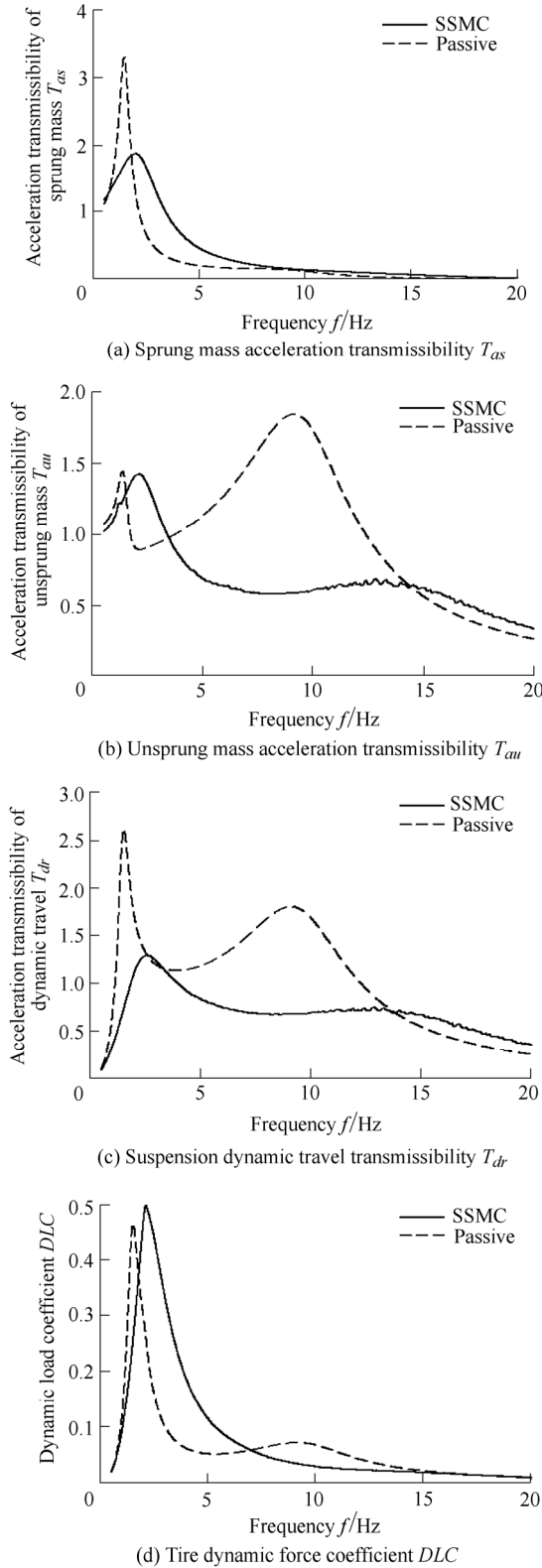
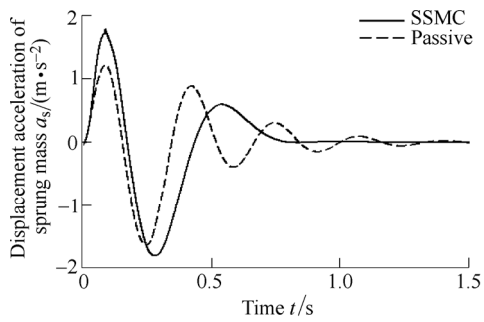


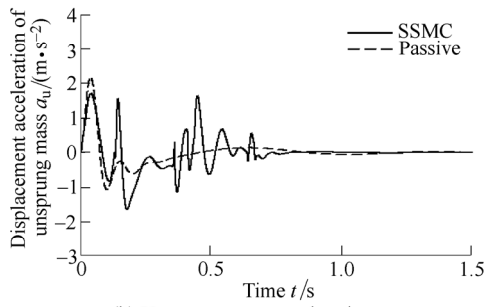
Fig. 8. Frequency domain response comparisons of SSMC-based MR and passive quarter-vehicle suspension systems under varied amplitude harmonic excitations



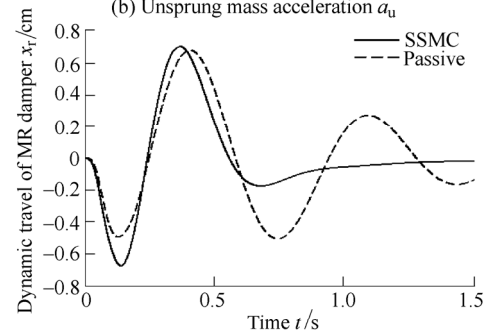
suspension performance but also the control robustness on vehicle load uncertainty. The passengers or goods of vehicle are often changing in real operation and the sprung mass difference between empty load and full load of a vehicle is usually larger, which will seriously affect the suspension control performance. Herein, the vehicle empty load sprung mass is assumed as  $m_{s0}=563$  kg, and its half load and full load sprung masses are 1.5 and 2 times of  $m_{s0}$ , the robustness of the proposed SSMC-based MR quarter-vehicle suspension system is further evaluated by comparing the suspension performance under above mentioned three kinds of load conditions.



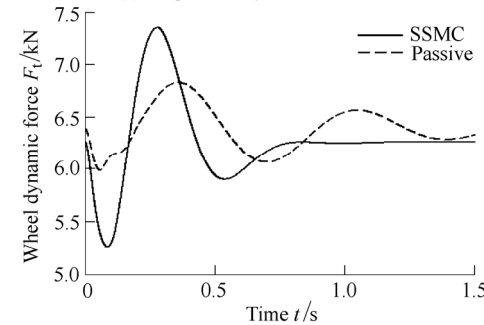
(a) Sprung mass acceleration  $a_s$



(b) Unsprung mass acceleration  $a_u$

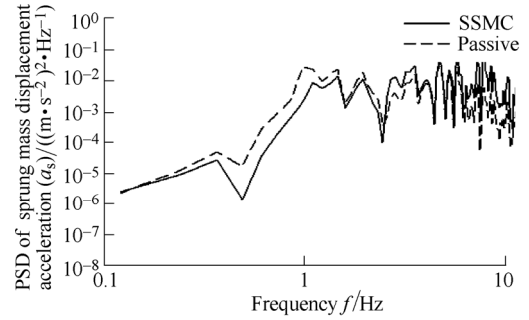


(c) Suspension dynamic travel  $x_r$

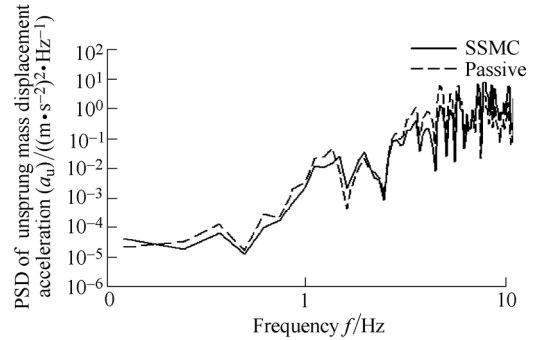


(d) Tire dynamic force  $F_t$

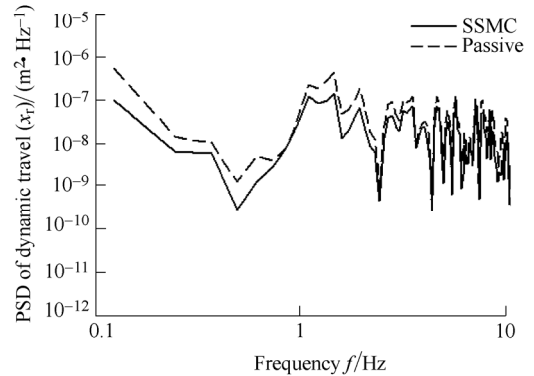
Fig. 9. Time domain transient response comparisons of SSMC-based MR and passive quarter-vehicle suspension systems under rounded pulse excitation



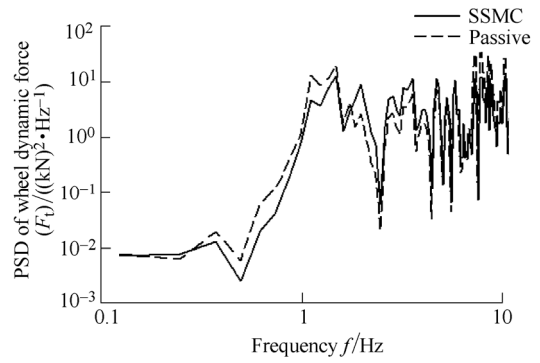
(a) Sprung mass acceleration  $a_s$



(b) Unsprung mass acceleration  $a_u$



(c) Suspension dynamic travel  $x_r$



(d) Tire dynamic force  $F_t$

Fig. 10. Response PSD comparisons of SSMC-based MR and passive quarter-vehicle suspension systems under real road measured random excitation

To analyze the robust performance, we further analyze the rates of associated performance indexes under empty load and full load benchmarked against that of half load, which is considered as normal load of the vehicle suspension. Herein, the robustness quantitative value is calculated with the average of above two rates, as follows

$$\sigma(i) = \frac{|\Delta X_e(i) / X_h(i)| + |\Delta X_f(i) / X_h(i)|}{2}, \quad (32)$$

where  $\sigma$  is the robustness quantitative value,  $i$  expresses the selected different performance indexes,  $X_h(i)$  is the performance index value under half load,  $\Delta X_e(i)$  and  $\Delta X_f(i)$  are the performance index variations under the empty and full loads with respect to the half load, respectively.

The frequency domain response comparisons of SSMC-based MR quarter-vehicle suspension system with empty, half and full vehicle loads are shown in Fig. 11, under the varied amplitude harmonic excitation in Eq. (30), and the system evaluation indexes are also chosen as the sprung mass displacement acceleration transmissibility  $T_{as}$ , unsprung mass displacement acceleration transmissibility  $T_{au}$ , suspension dynamic travel transmissibility  $T_{dr}$  and the tire dynamic load coefficient  $DLC$ . The results show that when the sprung mass  $m_s$  changes from empty load to full load, the sprung mass resonance frequency slightly decreases, and the responses of  $T_{as}$ ,  $T_{au}$ ,  $T_{dr}$  and  $DLC$  have good consistence and small relative change, as well as their magnitudes generally show slight decrease except for a little magnitude increase of  $T_{au}$  and  $T_{dr}$  in the low frequency band 0–1.5 Hz and the middle frequency band 5–15 Hz. The results further show that the robustness quantitative values of sprung mass resonance peaks for above  $T_{as}$ ,  $T_{au}$ ,  $T_{dr}$  and  $DLC$  are calculated as  $\sigma(T_{as})=1.9\%$ ,  $\sigma(T_{au})=6.6\%$ ,  $\sigma(T_{dr})=3.1\%$  and  $\sigma(DLC)=3\%$ , respectively, according to Eq. (32). The result thoroughly illustrates that the proposed SSMC-based MR quarter-vehicle suspension system has ideal robustness on vehicle load variation in the dominant frequency band of road vehicle.

The transient time domain response comparisons of the SSMC-based MR quarter-vehicle suspension system with empty, half and full vehicle loads are presented in Fig. 12, under the rounded pulse excitation in Eq. (31). It is not difficult to find that when the sprung mass  $m_s$  changes from empty load to full load, the response steady state time has only slight increase, and responses of  $a_s$ ,  $a_u$ ,  $x_r$  and  $F_t$  have good consistence and small relative change, as well as the peak magnitudes of  $a_s$  and  $F_t$  show slight decrease while the peak magnitude of  $x_r$  shows a little increase. Similarly, the robustness quantitative values of sprung mass resonance peaks for above  $a_s$ ,  $a_u$ ,  $x_r$  and  $F_t$  are calculated as 21.6%, 1%, 17.3% and 12.7%, respectively. The results further illustrate that the proposed SSMC-based MR quarter-vehicle suspension system has ideal robustness on the vehicle sprung mass variation in view of the road shock excitation.

In Fig. 13, the response PSD comparisons of the SSMC-based MR quarter-vehicle suspension system with empty, half and full vehicle loads are shown, under the real road measured random excitation<sup>[14, 17]</sup>, and it can be easily found that when the sprung mass  $m_s$  changes from empty load to full load, the PSD responses of  $a_s$ ,  $a_u$ ,  $x_r$  and  $F_t$  have good consistence and small relative change, and their

magnitudes show slight increase in the low frequency band. Furthermore, we choose the RMS of PSD value within the frequency range between 1–3 Hz, so as to evaluate the robustness performance under random excitation. Herein, the robustness performance index values are obtained as  $\sigma(a_s)=2.3\%$ ,  $\sigma(a_u)=5.1\%$ ,  $\sigma(x_r)=4.2\%$  and  $\sigma(F_t)=3.9\%$ , respectively, according to Eq. (32). The result shows that the proposed SSMC-based MR quarter-vehicle suspension system has ideal robustness on the vehicle load uncertainty.

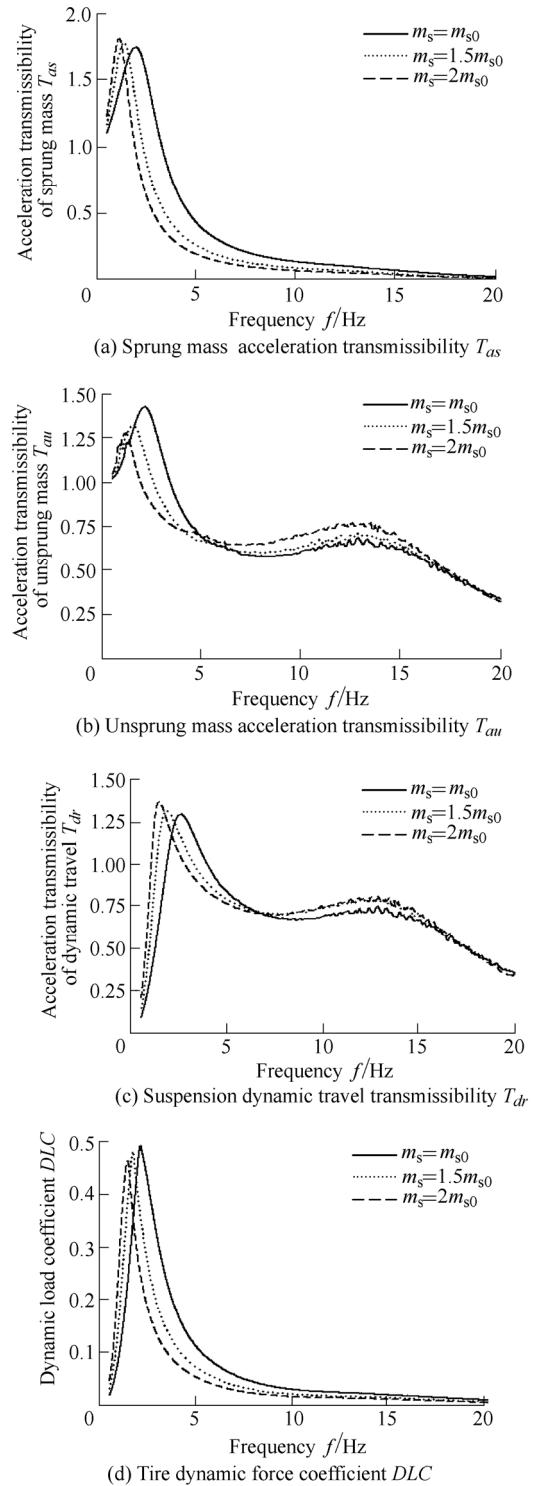
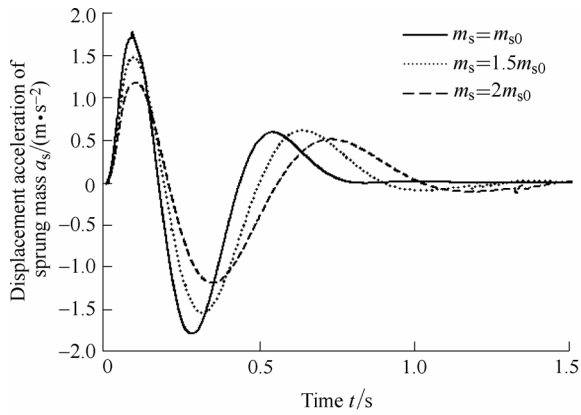
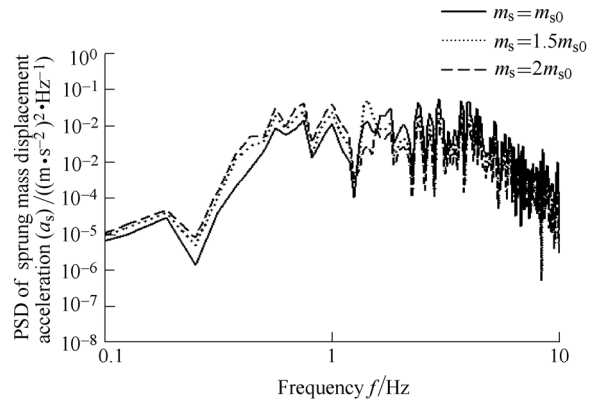


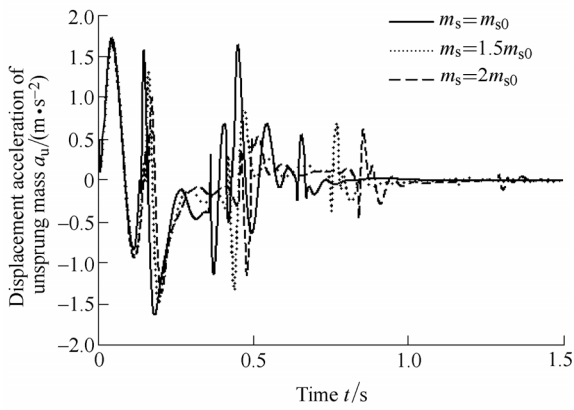
Fig. 11. Frequency domain response comparisons of SSMC-based MR quarter-vehicle suspension system with empty, half and full vehicle loads



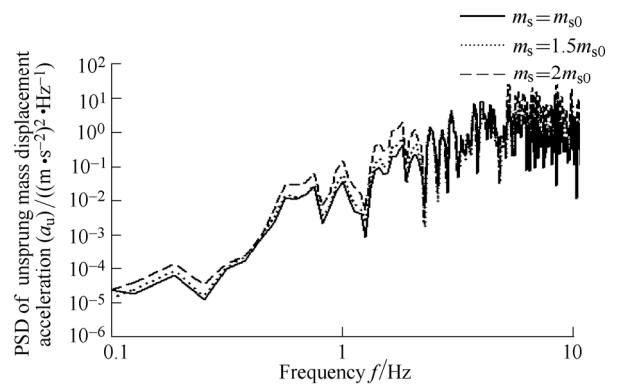
(a) Sprung mass acceleration  $a_s$



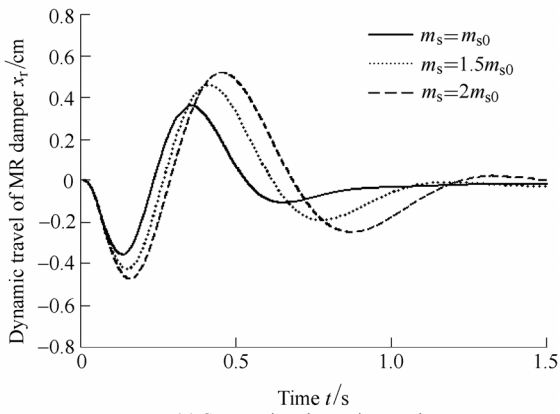
(a) Sprung mass acceleration  $a_s$



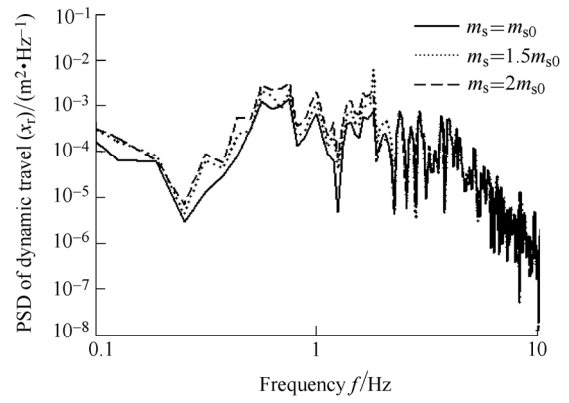
(b) Unsprung mass acceleration  $a_u$



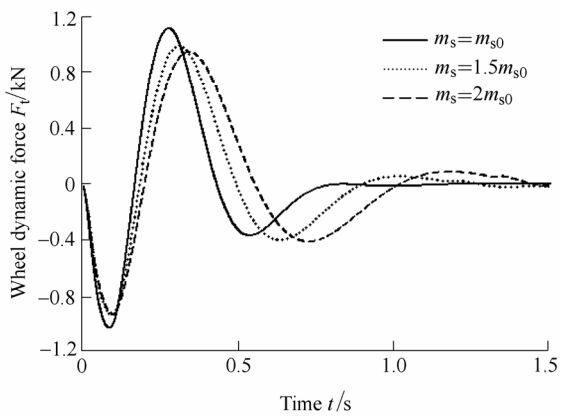
(b) Unsprung mass acceleration  $a_u$



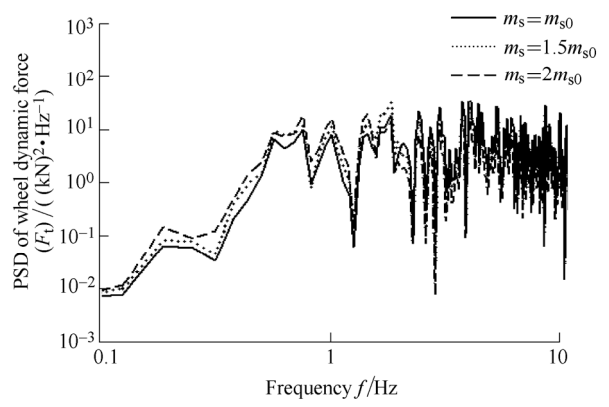
(c) Suspension dynamic travel  $x_r$



(c) Suspension dynamic travel  $x_r$



(d) Tire dynamic force  $F_t$



(d) Tire dynamic force  $F_t$

Fig. 12. Time domain transient response comparisons of SSMC-based MR quarter-vehicle suspension system with empty, half and full vehicle loads

Fig. 13. Response PSD comparisons of SSMC-based MR quarter-vehicle suspension system with empty, half and full vehicle loads

## 7 Conclusions

(1) In order to reasonably resolve the contradictory control requirements on the suspension damping for ride comfort and handling safety performances, and realize adaptive robust control on hysteresis nonlinearity and load uncertainty of the MR vehicle suspension, we derive the acquired control damping force and converting it to the direct drive current of the MR damper from the dynamic errors between the plant and skyhook-based reference suspension model system. The proposed SSMC-based MR quarter-vehicle suspension system establishes a solid theoretical foundation as the fundamental control scheme for the adaptive semi-active control study of MR full-vehicle suspension decoupled into four MR quarter-vehicle sub-suspension systems.

(2) The proposed SSMC reasonably combines the traditional sliding mode control, inverse model control and the idealized skyhook damping control. Thus the adaptive robust control on hysteresis nonlinearity and load uncertainty is realized. Meanwhile, the ideal ride comfort and handling safety performances of the MR vehicle suspension are obtained.

(3) The proposed modified Bouc-wen hysteretic  $F-v$  model and its inverse model, as well as the proposed continuous modulation filtering algorithm without phase shift are employed to derive the acquired direct drive current with high precision and continuous property, which can effectively decrease the harsh mechanical rub of piston motion and thus extending the service life of MR damper.

(4) The proposed three road excitations of varied amplitude harmonic, rounded pulse and road measured random signals are utilized to analyze the proposed SSMC-based MR quarter-vehicle suspension system. Thus it is verified systematically that the proposed SSMC can ideally realize the multi-objective suspension control performances above-mentioned.

(5) The proposed SSMC-based MR quarter-vehicle suspension system can be easily realized in real engineering application, because it acquires only in-time measured vertical motion displacements of the vehicle sprung and unsprung masses with reference to the road surface, while other variables can be calculated from the system model.

## References

- [1] MARGOLIS D L. Procedure for comparing passive, active, and semi-active approaches to vibration isolation[J]. *Journal of the Franklin Institute*, 1983, 315(4): 225–238.
- [2] ZHAO Yanshui, ZHOU Kongkang, LI Zhongxing, et al. Time Lag magnetorheological damper semi-active suspensions[J]. *Journal of Mechanical Engineering*, 2009, 45(7): 221–227. (in Chinese)
- [3] ZHU Maofei, CHEN Wuwei, ZHU Hui. Time-delay variable structure control for semi-active suspension based on magneto-rheological damper[J]. *Chinese Journal of Mechanical Engineering*, 2010, 12(46): 113–120.
- [4] LI Rui, YU Miao, CHEN Weiming, et al. Control of automotive suspensions vibration via magneto rheological damper[J]. *Journal*

- of Mechanical Engineering*, 2005, 41(6): 128–132. (in Chinese)
- [5] LEE H G, SUNG K G, CHOI S B, et al. Performance evaluation of a quarter-vehicle MR suspension system with different tire pressure[J]. *International Journal of Precision Engineering and Manufacturing*, 2011, 12(2): 203–210.
- [6] HONG K S, SOHN H C, HEDRICK J K. Modified skyhook control of semi-active suspensions: a new model, gain scheduling, and hardware-in-the-loop tuning[J]. *Journal of Dynamic Systems, Measurement, and Control*, 2002, 124: 158–167.
- [7] YOKOYAMA M, HEDRICK J K, TOYAMA S. A model following sliding mode controller for semi-active suspension systems with MR dampers[J]. *Proceedings of American Control Conference*, 2001, 4: 2652–2657.
- [8] YAO Jialing, ZHENG Jiaqiang, GAO Weijie, et al. Sliding mode control of vehicle semi-active suspension with magnetorheological dampers having polynomial model[J]. *Journal of System Simulation*, 2009, 21(8): 2400–2404. (in Chinese)
- [9] GUO Dalei, HU Haiyan, YI Jianqiang. Neural network control for a semi-active vehicle suspension with a magnetorheological damper[J]. *Journal of Vibration and Control*, 2004, 10(3): 461–471.
- [10] CHOI S B, LEE H S, PARK Y P.  $H_\infty$  control performance of a full-vehicle suspension featuring magneto-rheological dampers[J]. *Vehicle System Dynamics*, 2002, 38(5): 341–360.
- [11] SONG Hui, QIU Wei, WANG Enrong. The sliding model-following control for semi-active MR-vehicle suspension[C/CD]//*Processings of 2010 IEEE International Conference on Networking, Sensing and Control (IEEE ICNSC 2010)*, Chicago, USA, April 11–13, 2010.
- [12] WANG Enrong, SONG Hui, YAN Wei, et al. The hybrid sliding model-following control for semi-active MR-vehicle suspension: China, CN102004443A[P]. 2011-04-06.
- [13] WANG Wanjun, YING Liang, WANG Enrong. Comparison on models of controllable magneto-rheological dampers[J]. *Chinese Journal of Mechanical Engineering*, 2009, 45(9): 100–108. (in Chinese)
- [14] WANG Enrong, YING Liang, WANG Wanjun, et al. Semi-active control of vehicle suspension with MR-damper: Part I-controller synthesis and evaluation[J]. *Chinese Journal of Mechanical Engineering*, 2008, 21(1): 13–19.
- [15] WANG Enrong, YING Liang, WANG Wanjun, et al. Semi-active control of vehicle suspension with MR-damper: Part II-evaluation of suspension performance[J]. *Chinese Journal of Mechanical Engineering*, 2008, 21(2): 52–59.
- [16] WANG Enrong, YING Liang, WANG Wanjun, et al. Semi-active control of vehicle suspension with MR-damper: Part III-experimental validation[J]. *Chinese Journal of Mechanical Engineering*, 2008, 21(4): 93–100.
- [17] ZHANG Hailong, WANG Enrong, MIN Fuhong, et al. Skyhook-based semi-active control of full-vehicle suspension with magneto-rheological dampers[J]. *Chinese Journal of Mechanical Engineering*, 2013, 26(3): 511–518.
- [18] SPENCER B F, DYKE D J, SAIN K M, et al. Phenomenological model of a magnetorheological damper[J]. *Journal of Engineering Mechanics*, 1997, 123(3): 230–238.
- [19] WANG D H, LIAO Wei Hsin. Magneto-rheological fluids dampers: A review of parametric modeling[J]. *Smart Materials and Structures*, 2011, 20(2): 1–34.
- [20] SANKARANARAYANAN V, EMEKLI M E, GÜVENÇ B A, et al. Semiactive suspension control of a light commercial vehicle[J]. *IEEE/ASME Transactions on Mechatronics*, 2008, 13(5): 598–604.

## Biographical notes

ZHANG Hailong, born in 1988, is currently a PhD candidate at *School of Physics and Technology, Nanjing Normal University, China*. He received his master degree from *School of Electric and Automation Engineering, Nanjing Normal University, China*, in 2010. His research interests include the semi-active control for

implementing intelligent vehicle suspension with MR dampers.  
E-mail: zhl\_chosenone@163.com

WANG Enrong, obtained his BS and MS degrees in 1985 and 1988, respectively, both from *Southeast University, China* and obtained his PhD degree in 2006 from *Concordia University, Canada*. He joined *Nanjing Normal University* in 1988, where he is currently professor and dean of School of Electric and Automation Engineering. His research interests focus on the semi-active control for implementing intelligent vehicle suspension with MR dampers, and the related subjects in fields of electrical engineering and automation.  
Tel: +86-25-85481043; E-mail: erwang@njnu.edu.cn

ZHANG Ning, is currently a professor at *School of Physics and Technology, Nanjing Normal University, Nanjing, China*. His research interests focus on magnetic materials and magnetism, condensed matter and related area.  
E-mail: zhangning@njnu.edu.cn

MIN Fuhong, is currently a associate professor at *School of Electric and Automation Engineering, Nanjing Normal University, China*. Her research interests focus on the bifurcation and stability of discontinuous dynamic systems and its application in secure communication.  
E-mail: minfuhong@njnu.edu.cn

SUBASH Rakheja, is currently a professor of mechanical engineering at *Concordia University, Canada*. His research interests include advanced transportation systems and highway safety, human responses to workplace vibration, and driver-vehicle interactions.  
E-mail: rakheja@vax2.concordia.ca

SU Chunyi, is currently a professor of mechanical engineering at *Concordia University, Canada*. His research interests focus on automatic control theory and application about non-smooth dynamic system, hysteresis nonlinearities in smart actuators, robots.  
E-mail: chunyi.su@gmail.com